ЖЭТФ, 2006, том 130, вып. 4 (10), стр. 715–723

ENTROPY, FREE ENERGY AND PHASE TRANSITIONS IN THE LATTICE LOTKA – VOLTERRA MODEL

O. A. Chichigina*

Lomonosov Moscow State University
119992, Moscow, Russia

G. A. Tsekouras, A. Provata

Institute of Physical Chemistry
National Center for Scientific Research "Demokritos"
15310, Athens, Greece

Received April 3, 2006

A thermodynamic approach is developed for reactive dynamic models restricted to substrates of arbitrary dimensions, including fractal substrates. The thermodynamic formalism is successfully applied to the lattice Lotka – Volterra (LLV) model of autocatalytic reactions on various lattice substrates. Different regimes of reactions described as phases, and phase transitions are obtained using this approach. Predictions of the thermodynamic theory confirm extensive numerical kinetic Monte Carlo simulations on square and fractal lattices. Extensions of the formalism to multispecies LLV models are also presented.

PACS: 82.60.-s, 05.45.Df, 82.65.+r

1. INTRODUCTION

Nonlinear reactive processes restricted to low-dimensional supports have been under intensive investigation for the last thirty years, because of their importance for applications in physics, chemistry, biology, and ecology [1–13]. Low-dimensional systems are especially important in heterogeneous catalytic processes where reactions can only take place if the reactive species are adsorbed on the surface of the catalyst. They also give the possibility to answer fundamental questions about the behavior of open systems and about mechanisms of self-organization. To investigate the mechanisms of producing complexity and self-organization in reactive dynamics, several abstract models have been developed, which retain only the most important features for producing complexity [14–22].

The lattice Lotka – Volterra (LLV) model has attracted attention during the past years due to the large variety of patterns that it generates on low-dimensional support under variations of parameters and boundary conditions [21–26]. The LLV model involves two kinds of reacting molecules (X_1 and X_2) and empty lattice sites S. When two reactants X_1 and X_2 occupy two nearest-neighbor sites, X_1 can be transformed into X_2 with a probability k_s,

$$X_1 + X_2 \xrightarrow{k_s} 2X_2. \tag{1}$$

The reactant X_2 can desorb from the surface with a probability k_1 provided that there is a second empty site S in the neighborhood,

$$X_2 + S \xrightarrow{k_1} 2S. \tag{2}$$

X_1 may adsorb on the surface from a bulk phase with a probability k_2 provided that another X_1 is already adsorbed on a neighboring site,

$$S + X_1 \xrightarrow{k_2} 2X_1. \tag{3}$$

In this scheme, the particles react when they are attached to the lattice and do not diffuse to nearest neighbor empty sites. In the traditional mean-filed (MF) approach, the LLV system can be described by the dynamical system [22, 23]

*E-mail: chichigina@hotmail.com, chichigina1@yandex.ru

$$\frac{dx_1(t)}{dt} = k_2 x_1 s - k_s x_1 x_2, \tag{4a}$$

$$\frac{dx_2(t)}{dt} = k_s x_2 x_1 - k_1 x_2 s, \tag{4b}$$

$$\frac{ds(t)}{dt} = k_1 x_2 s - k_2 x_1 s, \tag{4c}$$

where the variables $x_1(t), x_2(t)$, and s are the partial concentrations of particles X_1, X_2, and empty sites S. The notation hereafter follows Ref. [23]. Diffusion terms are not included in Eq. (4) because the particles are not allowed to diffuse. The LLV construction immediately implies that there is a constant of motion:

$$C = x_1 + x_2 + s = 1. \tag{5}$$

This constant C corresponds to the total coverage of each lattice site, which either contains particles (X_1 or X_2) or is empty (S). We can set $C = 1$. Using Eq. (5), we can reduce the number of variables to two, x_1 and x_2:

$$\frac{dx_1(t)}{dt} = k_2 x_1 \left(1 - x_1 - \frac{k_2 + k_s}{k_2} x_2\right), \tag{6a}$$

$$\frac{dx_2(t)}{dt} = -k_1 x_2 \left(1 - x_2 - \frac{k_1 + k_s}{k_1} x_1\right). \tag{6b}$$

The behavior of this system is closely related to the behavior of the original Lotka–Volterra system, developed for the description of predator–prey dynamics [1, 2], but the latter system is not suitable for realization on a lattice because it does not take the spatial constraints into account (constant number of total, empty, and occupied lattice sites). The dynamical system in (6a) has four fixed points, three of which are saddle points and one is a center. The saddle points are $(0,0)$, $(0,1)$, $(1,0)$, and the center is $(k_1/(k_1+k_2+k_s), k_2/(k_1+k_2+k_s))$. The center is surrounded by a continuum of closed trajectories, whose amplitudes depend solely on the initial conditions [22].

Equations (4) and (6a) describe an idealistic model where each particle reacts with the mean field of all other particles in the system. This is not the case in heterogeneously catalyzed systems, where the particles are attached to the substrate sites and can only react with their nearest neighbors. These local interactions induce important spatiotemporal fluctuations that cannot be adequately described by the MF equations. To study such minimal-complexity models, to explore the spatiotemporal structures they demonstrate when restricted to low-dimensional substrates, and to understand the qualitative and quantitative deviations from the mean-field behavior, computer simulations have been extensively used in recent years [10–12, 14–20].

Although the MF equations predict oscillatory behavior for all values of the kinetic parameters, kinetic Monte Carlo (KMC) simulations of the LLV model have demonstrated either oscillatory behavior or poisoning by one of the three species, depending on the substrate dimension D and the kinetic constants k_s, k_1, and k_2 [23]. The main purpose of this work is to describe the transitions of the LLV system from oscillatory to poisoning regimes and back as a kind of phase transitions, according to the laws of thermodynamics. To develop the thermodynamic approach, we first need to introduce the effective temperature T, energy U, and entropy S as functions of D, k_s, k_1, k_2. Then we can define the free energy F and analyze its dependence on the dimension and kinetic constants as order parameters.

In the next section, we introduce the thermodynamic approach to reactive dynamics and define the potential and kinetic energy, the effective temperature, the entropy, and the free energy. In Sec. 3, we present thermodynamic calculations for the LLV system at various parameter values. In Sec. 4, we compare the thermodynamics with numerical KMC results on the LLV system. In Sec. 5, we generalize the thermodynamic formalism to multispecies LLV systems. Finally, in the concluding section, we recapitulate our main results and discuss open problems.

2. THERMODYNAMIC FORMALISM

A. The energy

To develop the thermodynamic formalism, we first describe the qualitative difference between the three species by a quantitative difference of three energy states. We consider a Brownian particle that can move in three potential wells under the influence of thermal noise. Each potential well corresponds to one of the species as illustrated in Fig. 1 and the whole system corresponds to one lattice site. Thus, one lattice site can change its state from X_1 to X_2 and S as depicted in Fig. 1.

The potential energy of a well is connected with the escape probability for one time step (or kinetic constant) by the Kramers formula [27]:

$$k_2 = \exp\frac{U_s}{kT}, \tag{7}$$

$$k_1 = \exp\frac{U_2}{kT}, \tag{8}$$

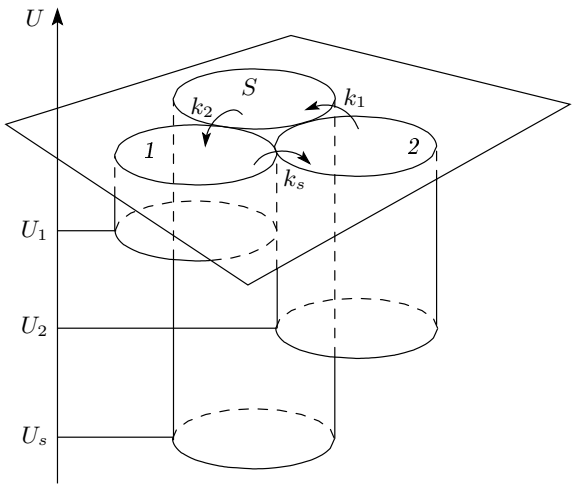

Fig. 1. The LLV model represented as a Brownian particle transition from one potential well to another

$$k_s = \exp \frac{U_1}{kT}, \tag{9}$$

where k is the Boltzmann constant. From Eqs. (7)–(9), the energies U_s, U_1, and U_2 can be expressed as functions of the k_i and the temperature.

B. Steady states

To find the average energy, we calculate the steady probability distribution P_s, P_1, and P_2 under the normalization condition

$$P_s + P_1 + P_2 = 1. \tag{10}$$

We consider the Markov matrix of transitions for one step, $\hat{B} = \{b_{ij}\}$, were b_{ij} is the probability of transition to state i from state j, as

$$\hat{B} = \begin{pmatrix} b_{ss} & b_{s1} & b_{s2} \\ b_{1s} & b_{11} & b_{12} \\ b_{2s} & b_{21} & b_{22} \end{pmatrix}. \tag{11}$$

These probabilities are defined in terms of the kinetic constants as

$$\hat{B} = \begin{pmatrix} 1-k_2 & 0 & k_1 \\ k_2 & 1-k_s & 0 \\ 0 & k_s & 1-k_1 \end{pmatrix}. \tag{12}$$

The eigenvalues λ may be obtained from the equation

$$\hat{B} \begin{pmatrix} P_s \\ P_1 \\ P_2 \end{pmatrix} = \lambda \begin{pmatrix} P_s \\ P_1 \\ P_2 \end{pmatrix}. \tag{13}$$

With $1 - \lambda = \beta$, Eq. (13) transforms into the equation

$$\det \hat{C} = 0, \tag{14}$$

where the matrix $\hat{C}$ is

$$\hat{C} = \begin{pmatrix} \beta - k_2 & 0 & k_1 \\ k_2 & \beta - k_s & 0 \\ 0 & k_s & \beta - k_1 \end{pmatrix}. \tag{15}$$

From Eq. (14), we find three eigenvalues: $\lambda_0 = 1$, which corresponds to the steady state, and $\lambda_{1,2} < 1$. Substituting λ_0 in Eq. (13), we obtain the steady probability distribution as

$$P_2 = \frac{\xi}{k_1}, \quad P_s = \frac{\xi}{k_2}, \quad P_1 = \frac{\xi}{k_s}, \tag{16}$$

where

$$\xi = \frac{k_s k_1 k_2}{k_s k_1 + k_1 k_2 + k_2 k_s}. \tag{17}$$

C. Average energy and temperature

Using Eqs. (7)–(9) and (16), we can find the average potential energy for one Brownian particle, which represents one lattice site «jumping» between the states X_1, X_2, and S, as

$$\langle U \rangle = \sum_i U_i P_i = kT\xi \left(\frac{\ln k_2}{k_2} + \frac{\ln k_1}{k_1} + \frac{\ln k_s}{k_s} \right) = kT\xi \sum_j \frac{\ln k_j}{k_j}. \tag{18}$$

The average kinetic energy is equal to $kT/2$, in accordance with the theorem on equal distribution of energy among the degrees of freedom, because the motion of the imaginary particle is one-dimensional.

The temperature in our description is not a real temperature, but an effective one. It characterizes the intensity of the Brownian particle motion, which is regarded as a diffusion-like process. Here, it is not possible to define the temperature in the usual way through the entropy [28, 29], because the state is not equilibrium [30]. However, its dependence on the kinetic constants can be assumed to be approximately linear due to the diffusive character of motion, and can be described by the Einstein formula $\langle x^2 \rangle = 2Dt$ [31]. It is known that $\langle x^2 \rangle$ is proportional to the probability of a fixed step in a fixed time, while the diffusion coefficient D is proportional to the temperature. Therefore, the temperature can be assumed directly proportional to the sum of the transition probabilities:

$$T = \tau(k_s + k_1 + k_2). \tag{19}$$

The constant τ is defined in terms of time steps.

D. The entropy

To define the entropy, we use the information interpretation, which is useful in complex systems and gives good agreement with experiments [32–34]. The uncertainty of one transition with a probability k_j is

$$I(k_j) = k_j \ln k_j + (1 - k_j) \ln (1 - k_j). \qquad (20)$$

The entropy for one interaction is defined by the sum of all transitional uncertainties, all of which are multiplied by two probabilities: the probability that the particle under consideration is in the state to open this transition for a neighbor particle, and the probability that this neighboring particle is in the state for this transition. Then the entropy for one site in the lattice is equal to the entropy for one interaction multiplied by the number of all possible combinations of particles interacting with the particle under consideration. It is $nn!$, where nn is the average number of nearest neighbors. The particles are not indistinguishable, they are marked by the special place they occupy on the lattice.

It is not easy to find the number of nearest neighbors, or coordination number, nn [35]. In the first-order approximation and for hypercubic lattices of dimension D, the average number of nearest neighbors is $2D$. It varies for other types of lattices: triangular, polygonal, etc. It also varies significantly due to fluctuations around the average for random and fractal lattices. In lattice dynamics in general, the coordination number also has local fluctuations, which may contribute significantly to the creation of patterns and local structures.

In the first-order approximation, however, we can write the entropy for all kinds of lattices as

$$S = -nn!k[I(k_1)P_2P_s + I(k_2)P_sP_1 + I(k_s)P_1P_2], \quad (21)$$

where $nn = 2D$ for hypercubic lattices and is calculated numerically for fractal lattices.

E. Free energy

We can now define the free energy as the sum of the potential, kinetic, and entropy terms:

$$F(k_1, k_2, k_s, D) = \langle U \rangle + kT/2 - ST. \qquad (22)$$

In the case where $D = 2$ (square lattice), the free energy dependence on one of the k_j has a maximum, which defines two phases: oscillations and poisoning. This interpretation, as described above, is semiphenomenological.

3. THERMODYNAMIC CALCULATIONS OF THE LLV MODEL

Using the thermodynamic formalism developed above, we now attempt to describe the phase transition (from poisoned to nonpoisoned states) of the LLV system. To validate our low-dimensional results, we compare them with Monte Carlo simulations in Ref. [23]. In this reference, the authors show that small values, e.g., of k_2 lead to poisoning by X_1. The mechanism described in Ref. [23] is as follows: because of small k_2, the X_1 particles are produced very infrequently; as a result, X_2 attains a very low concentration and at a certain point, S can almost dominate the lattice by destroying all X_2. At the same time, the remaining clusters of X_1 start to grow and gradually invade the entire lattice. By the same mechanism, when low k_1 are considered, the S states poison the lattice, and similarly for low k_s, the X_2 states dominate. In intermediate cases, where k_2 is small but k_s is also sufficiently small, the small cluster of X_2 can be left inside X_1-dominated regions. Only small clusters (when k_s is small) can survive and do not reach the S-region. Then X_2 grows and we have X_2-poisoning.

Because the kinetic constants k_j are related to poisoning by the corresponding particles, we can consider the kinetic constants as order parameters. A phase transition occurs when the free energy, which is a function of the k_j, passes a maximum. Low values of k_j (at the left-hand side of the maximum) correspond to poisoning by the respective particles, while large values of k_j correspond to oscillations. This way, we can define the final, steady-state behavior of the system for all values of the kinetic constants.

Figure 2 illustrates the free energy $F(k_2)$ at $k_1 = 0.8$

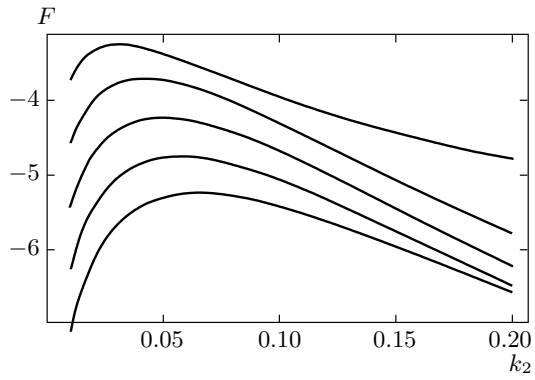

Fig. 2. The free-energy dependence on k_2 for a two-dimensional lattice at $k_1 = 0.8$ and $k_s = 0.1$, 0.3, 0.5, 0.7, 0.9 from top down

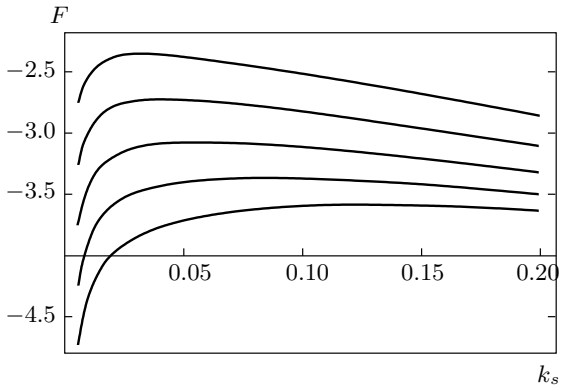

Fig. 3. The free-energy dependence on k_s for a two-dimensional lattice at $k_2 = 0.05$ and $k_1 = 0.5$, 0.6, 0.7, 0.8, 0.9 from top down

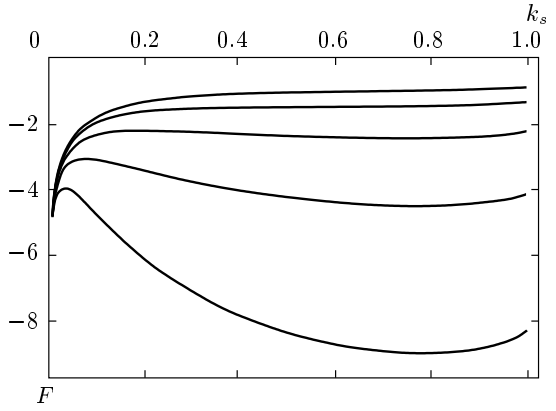

Fig. 4. The free-energy dependence on k_s for different numbers of nearest neighbors $nn = 2$, 2.5, 3, 3.5, 4 from top down at $k_1 = 0.6$, $k_2 = 0.4$

and different values of $k_s = 0.1$, 0.3, 0.5, 0.7, 0.9 from top down, for a square lattice. We can see that for $k_2 = 0.05$, which is considered in the next section, X_1-poisoning occurs for $k_s > 0.2$. The higher the values of k_2, the less poisoning is observed. At $k_2 = 0.075$, we have poisoning only for $k_s > 0.8$, and there is no poisoning at $k_2 = 0.1$.

To decide whether X_2-poisoning is possible, we consider $F(k_s)$, presented in Fig. 3 for the same lattice, $k_2 = 0.05$, and different values of k_1. Poisoning is only observed at $k_s = 0.1$ and for large values of $k_1 > 0.6$. These results are also presented in Fig. 8 for comparison with numerical KMC results.

The dimensionality also defines the shape of the free-energy dependence, and we therefore analyze the influence of the substrate dimensionality in autocatalytic processes. As the substrate dimensionality decreases, the free-energy maximum moves right and finally disappears, such that more poisoning states emerge. This is partly due to the dependence of the number of neighbors on the dimensionality.

Figure 4 presents the free energy $F(k_s)$ for the same kinetic constants and for different numbers of nearest neighbors nn; $nn = 2$ corresponds to the one-dimensional case and $nn = 4$ to the two-dimensional lattice. For small dimensions, the system is poisoned for all values of the kinetic constants.

In particular, in $D = 1$, oscillations are impossible. This becomes obvious from the shape of the free energy, which has no turning (maximum) points for any values of k_1, k_2 or k_s. This is shown in Fig. 5 for $F(k_s)$ at $k_2 = 0.6$ and different values of k_1. Some oscillations could have been possible only for very small k_1, in which case we expect poisoning by X_2. But if we

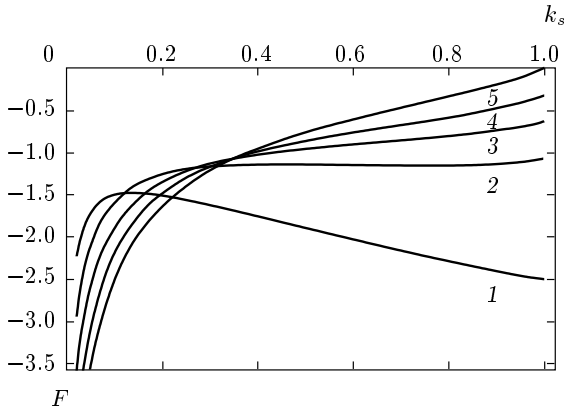

Fig. 5. The free-energy dependence on k_s for a one-dimensional lattice at $k_2 = 0.6$ and $k_1 = 0.1$ (*1*), 0.3 (*2*), 0.5 (*3*), 0.7 (*4*), 0.9 (*5*)

consider $F(k_1)$, this small k_1 is on the left-hand side of the maximum showing poisoning by S. The same results, for $D = 1$, were also obtained in [22] using KMC simulations and theoretical arguments.

4. COMPARISON WITH KINETIC MONTE CARLO SIMULATIONS

In [23], a set of LLV simulations was performed with very low values of k_2 ($k_2 = 0.05$ and $k_2 = 0.075$) at different values of k_1 and k_s for fractal ($D = 1.893$) and two-dimensional square lattice substrates. In this work, we produced new sets of results for $k_2 = 0.05$ and $k_2 = 0.1$ using a speeded version of the KMC algorithm in [23]. The KMC scheme used here is as follows.

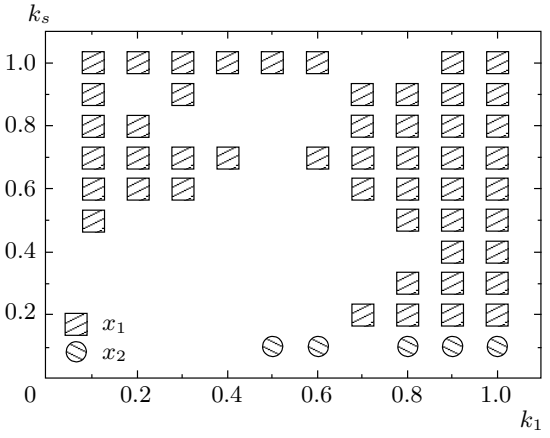

Fig. 6. Numerical results. Poisoning states for $k_2 = 0.05$. The simulations were performed on a two-dimensional square lattice substrate

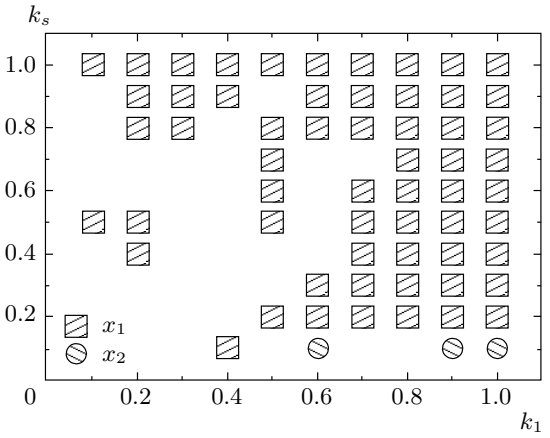

Fig. 7. Numerical results. Poisoning states for $k_2 = 0.05$. The simulations were performed on a random fractal substrate with $D = 1.893$

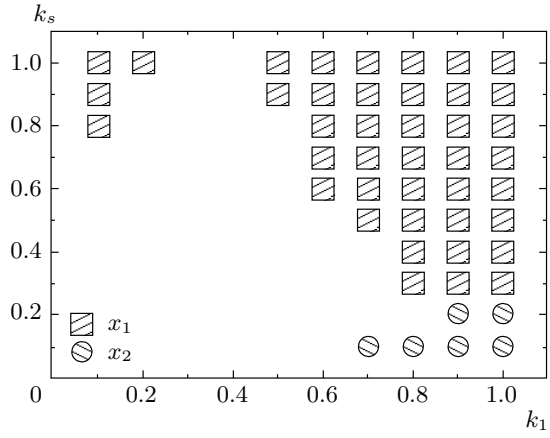

Fig. 8. Thermodynamic results. Poisoning states for $k_2 = 0.05$ on a two-dimensional square lattice substrate

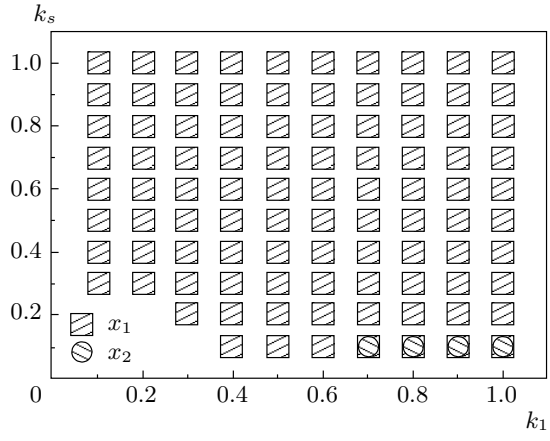

Fig. 9. Thermodynamic results. Poisoning states for $k_2 = 0.05$ on a random fractal substrate with $D = 1.893$

1. At each elementary time step (ETS) of the KMC procedure, one site of the lattice is chosen at random.

2. One of the nearest neighbors is also selected.

3. If the originally chosen site is X_1 and the selected neighbor is X_2, then the chosen site changes to X_2 with the probability $p_s = k_s/\max(k_1, k_2, k_s)$. If the originally chosen site is X_2 and the selected neighbor is S, then the chosen site changes to S with the probability $p_1 = k_1/\max(k_1, k_2, k_s)$. If the originally chosen site is S and the selected neighbor is X_1, then the chosen site changes to X_1 with the probability $p_2 = k_2/\max(k_1, k_2, k_s)$. Otherwise, the system remains unchanged.

4. The algorithm returns to step 1.

This particular choice of the probabilities considerably speeds the algorithm because at least one of the three processes takes place with probability 1, while the other two have relative probability weights. One Monte Carlo step (MCS) is finished after the number N of ETS steps equal to the number of substrate (active) lattice sites. Thus, at each MCS, each lattice site has reacted once on average. We note that due to the difference in this speeded version of the algorithm, the results in Figs. 6 and 7 do not correspond to those in Ref. [23].

Comparison of Fig. 6 with Fig. 8 and Fig. 7 with Fig. 9 demonstrates qualitative agreement of the KMC results with the corresponding thermodynamic approximation, for small values of $k_2 = 0.05$. The same KMC simulations were performed for $k_2 = 0.1$ (Figs. 10 and 12). Here, much less poisoning is observed both

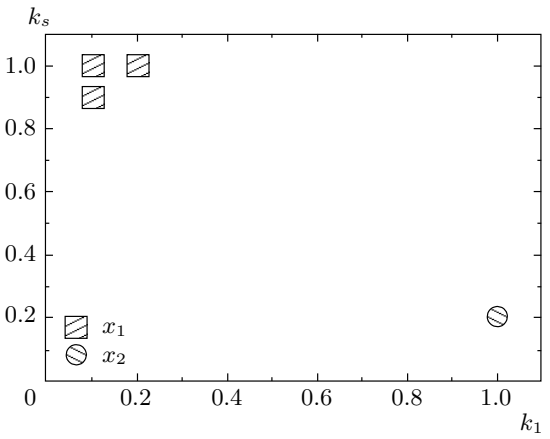

Fig. 10. Numerical results. Poisoning states for $k_2 = 0.1$. The simulations were performed on a two-dimensional square lattice substrate

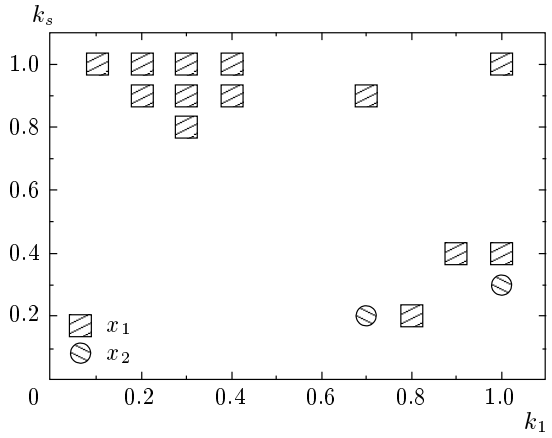

Fig. 12. Numerical results. Poisoning states for $k_2 = 0.1$. The simulations were performed on a random fractal substrate with $D = 1.893$

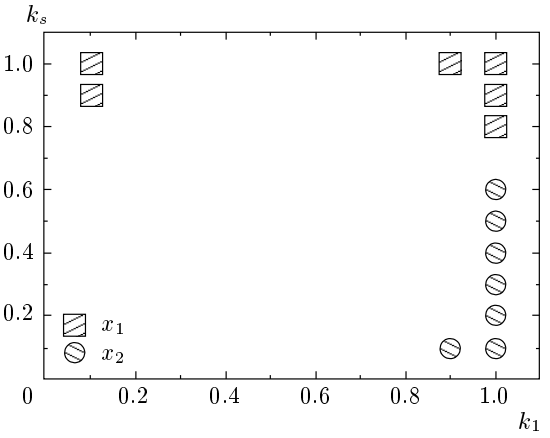

Fig. 11. Thermodynamic results. Poisoning states for $k_2 = 0.1$ on a two-dimensional square lattice substrate

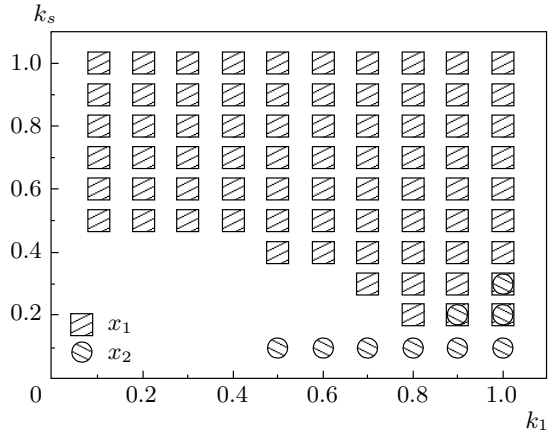

Fig. 13. Thermodynamic results. Poisoning states for $k_2 = 0.1$ on a random fractal substrate with $D = 1.893$

thermodynamically and numerically, except for poisoning at relatively high values of k_1 and k_s in the random fractal substrate (thermodynamic results).

From Figs. 6–13, both approaches show that the X_1-poisoning states are more favored on fractal lattices for identical kinetic constants. As k_s and k_1 increase, more poisoning states emerge for both fractal and two-dimensional lattices. The thermodynamic formula can also predict X_2-poisoning for small k_s and large k_1 values, the mechanism of which is described in Sec. 3.

For the fractal support with $D_f = 1.893$, the average number of nearest neighbors was calculated numerically as $nn = 3.315$, which is less than the number obtained using the approximation $nn = 2D = 2 \cdot 1.893 = 3.786$. This leads to more poisoning in the thermodynamic approach, and we used the numerically calculated nn as more precise.

This first approach to thermodynamic modeling of chemical dynamics achieves good agreement with numerical data. Some disagreement can be explained by the following phenomenological approximations used in the thermodynamics approach: a) We have calculated the average energy and entropy using steady-state probability distributions, which do not correspond to poisoning but are nevertheless used to find poisoning states as well as oscillatory regimes. b) For the energy calculations, we did not take into account that transitions depend on neighboring sites. Instead, we assumed

that interactions influence only the entropy. c) For fractal substrates, we used the approximate (numerically calculated) average number of neighbors. d) All thermodynamic parameters in our model are effective and cannot therefore be measured experimentally. Instead, they are introduced as functions of the kinetic constants using phenomenological interpretations.

Another source of disagreement between the thermodynamic approach and the KMC simulations is the statistical fluctuations in the simulations, which is especially important for fractal substrates. For example, some poisoning states can be achieved only asymptotically, after very long simulations times, while numerical experiments have a finite time of calculation. Some additional poisoning is possible because of limited lattice sizes (finite-size effects).

In the case of one-dimensional systems, both thermodynamic and KMC approaches agree, predicting poisoning for all values of the kinetic constants [22].

5. GENERALIZATION FOR MULTISPECIES LLV SYSTEMS

The entire formalism presented in Sec. 2 can be generalized to the case of M species. We consider the set of M transitions

$$X_i + X_{i+1} \xrightarrow{k_i} 2X_{i+1}, \quad i = 1, \ldots, M \tag{23}$$

with the corresponding kinetic constants k_i. All parameters have the cyclic symmetry: $A_{M+j} = A_j$.

The potential energies considered as functions of the k_i and the temperature are given by

$$U_i = kT \ln k_i < 0. \tag{24}$$

The steady probability distribution corresponds to

$$P_i = \frac{\xi}{k_i}, \tag{25}$$

where

$$\xi = \left(\sum_{i=1}^{M} \frac{1}{k_i} \right)^{-1}. \tag{26}$$

The average potential energy for one particle is estimated as

$$\langle U \rangle = \sum_i U_i P_i = kT\xi \sum_i \frac{\ln k_i}{k_i}. \tag{27}$$

The temperature can be generalized as

$$T = \tau \sum_i k_i, \tag{28}$$

while the entropy takes the form

$$S = -nn!k \sum_i I(k_i) P_i P_{i+1}, \tag{29}$$

where $I(k_i)$ is defined in Eq. (20).

In the case of many species, the dependence on the initial conditions becomes more important. Poisoning by several species is possible in this case. But the main tendency indicated by numerical simulations is an increase in poisoning states. This can also be obtained qualitatively from our thermodynamic theory. The entropy is bilinear in the probabilities, Eq. (29), and the average energy is linear, Eq. (27). As the number of species M increases, the steady-state probabilities decrease due to normalization. Thus, the effect of higher M is the same as decreasing the dimensionality D, leading to poisoning.

6. CONCLUSIONS

The thermodynamic approach can be useful in nonlinear reactive systems restricted to low-dimensional supports, because it allows considering transitions from chemical oscillations to poisoning regimes and back as phase transitions induced by the presence of the support. The main idea is to introduce an imaginary Brownian particle whose energies correspond to different kinds of reacting species. The potential energy can be defined through the kinetic constants using the Kramers formula. The average kinetic energy can be obtained from the theorem on equal distribution of energy among all degrees of freedom. The temperature can be estimated according to the Einstein diffusion equation. The entropy can be written as a measure of uncertainty in its informational interpretation. Introducing effective thermodynamical parameters allows defining the free energy in terms of the kinetic constants. The maximum of this free energy function separates the poisoning and oscillatory regimes. Taking relatively small values of a kinetic constant leads to poisoning by the corresponding species.

The new thermodynamic approach allows direct investigation of the influence of the substrate dimensions. Within this formalism, the behavior of the LLV model was considered when realized on square-lattice and fractal substrates. For the LLV model, it was shown that the lower the dimensionality of the substrate, the higher the possibility of poisoning. For one-dimensional systems, there are no oscillatory regimes. All thermodynamic results have been confirmed by numerical kinetic Monte Carlo simulations.

Generalizations of this theory can give new predictions of reactive phenomena that have not been studied yet, such as more complex dynamical mechanisms, higher or lower (fractal) dimensions, and mechanisms with many species involved.

All thermodynamic results qualitatively conform with computer simulations. Thus, the proposed thermodynamic approach can be considered a first approximation and a first step towards elaborating a thermodynamic theory of nonlinear dynamical systems restricted to low-dimensional supports.

O. Ch. gratefully acknowledges financial support and a research fellowship from the NATO Science fellowships program. G. A. T. and A. P. gratefully acknowledge financial support from the European Union under contract EPEAEK/PYTHAGORAS 70/3/7357.

REFERENCES

1. A. J. Lotka, P. Natl. Acad. Sci. USA **6**, 410 (1920).
2. V. Volterra, *Lecons sur la Theorie Mathematique de la Lutte Pour la Vie*, Gauthier-Villars, Paris (1931).
3. G. Nicolis and I. Prigogine, *Self-organization in Nonequilibrium Systems*, Wiley, New York (1977).
4. G. Ertl, Science, **254**, 1750 (1991).
5. J. Wintterlin, Adv. Catal. **45**, 131 (2000).
6. R. Imbihl and G. Ertl, Chem. Rev. **95**, 697 (1995).
7. C. Voss and N. Kruse, Ultramicroscopy **73**, 211 (1998).
8. J. D. Murray, *Mathematical Biology*, Springer, Berlin (1993).
9. R. Monetti, A. Rozenfeld, and E. Albano, Physica A **283**, 52 (2000).
10. T. Antal, M. Droz, A. Lipowski, and G. Odor, Phys. Rev. E **64**, 036118 (2001).
11. J. E. Satulovsky and T. Tome, J. Math. Biol. **35**, 344 (1997).
12. B. Spagnolo, M. Cirone, A. La Barbera, and F. de Pasquale, J. Phys.: Condens. Matter **14**, 2247 (2002).
13. G. Theraulaz, E. Bonabeau, S. C. Nicolis, R. V. Sole, V. Fourcassie, S. Blanco, R. Fournier, J. L. Jolly, P. Fernandez, A. Grimal, P. Dalle, and J. L. Deneubourg, P. Natl. Acad. Sci. USA **99** (15), 9645 (2002).
14. R. M. Ziff, E. Gulari, and Y. Barshad, Phys. Rev. Lett. **56**, 2553 (1986).
15. E. V. Albano and J. Marro, J. Chem. Phys. **113**, 10279 (2000).
16. M. Tammaro and J. W. Evans, J. Chem. Phys. **108**, 762 (1998).
17. D. J. Liu and J. W. Evans, Phys. Rev. Lett. **84**, 955 (2000).
18. Y. De Decker, F. Baras, N. Kruse, and G. Nicolis, J. Chem. Phys. **117**, 10244 (2002).
19. V. P. Zhdanov, Phys. Rev. E **60**, 7554 (1995).
20. V. P. Zhdanov, Surf. Sci. **426**, 345 (1999).
21. L. Frachebourg, P. L. Krapivsky, and E. Ben-Naim, Phys. Rev. E **54**, 6186 (1996).
22. A. Provata, G. Nicolis, and F. Baras, J. Chem. Phys. **110**, 8361 (1999).
23. G. A. Tsekouras and A. Provata, Phys. Rev. E **65**, 016204 (2002).
24. A. Provata and G. A. Tsekouras, Phys. Rev. E **67**, 056602 (2003).
25. C. Anteneodo, Eur. Phys. J. B **42**, 271 (2004).
26. A. V. Shabunin, A. Efimov, G. A. Tsekouras, and A. Provata, Physica A **347**, 117 (2005).
27. H. A. Kramers, Physica **7**, 284 (1940).
28. L. D. Landau and E. M. Lifshits, *Statisticheskaja fizika*, Nauka, Moscow (1986).
29. H. Haken, *Information and Selforganization*, Springer-Verlag, Berlin, Heidelberg, New York (1988).
30. J. Hirshfelder, F. Curtiss, and R. Bird, *Molecular Theory of Gases and Liquids*, Wiley, New York (1964).
31. R. L. Stratonovich, *Topics in the Theory of Random Noise*, Gordon and Breach, New York (1963).
32. R. L. Stratonovich, *Teorija Informacii*, Sovetskoe radio, Moscow (1975).
33. O. A. Chichigina, JETP **89**, 30 (1999).
34. O. A. Chichigina, JETP **95**, 1092 (2002).
35. G. Hummer, S. Garde, A. E. Garcia, A. Pohorille, and L. R. Pratt, P. Natl. Acad. Sci. USA **93**, 8951 (1996).